IRAQI JOURNAL OF MATERIALS
Volume (4) Issue (2) April-June 2025, pp. 69-74

Cadmium Manganite Nanostructures Synthesized by DC Reactive Co-Sputtering

Mauro J. Lovato, Alessandro Puerto, Nicola Gallinari

Department of Metallurgy and Materials Engineering, Faculty of Engineering, University of Malta, Msida, MALTA

Abstract
In this work, an attempt to prepare cadmium manganite ($CdMn_2O_4$) nanostructures is presented. These nanostructures were prepared by reactive magnetron co-sputtering technique. The cadmium and manganese targets were mounted in a geometrical configuration allowing to achieve the stoichiometry of the prepared compound. The effect of $Ar:O_2$ mixing ratio on the structural characteristics of the prepared nanostructures was introduced. The growth of crystal planes in the prepared samples could be reasonably controlled by tuning the operation parameters and preparation conditions. The structural characterization showed that the prepared nanostructures were highly pure.

Keywords: $CdMn_2O_4$; Nanostructures; Magnetron sputtering; Reactive sputtering
Received: 24 January 2025; **Revised:** 12 March 2025; **Accepted:** 27 March 2025; **Published:** 1 April 2025

1. Introduction

Cadmium manganite ($CdMnO_3$) nanostructures have garnered significant attention in recent years due to their unique structural, electronic, and magnetic properties, which make them promising candidates for applications in spintronics, catalysis, and energy storage devices [1-3]. The DC reactive magnetron co-sputtering technique is a versatile and efficient method for synthesizing high-quality $CdMnO_3$ nanostructures with controlled composition and morphology. This technique involves the simultaneous sputtering of cadmium (Cd) and manganese (Mn) targets in a reactive oxygen (O_2) environment, enabling the formation of cadmium manganite thin films or nanostructures with precise stoichiometry and structural uniformity [4-6].

One of the key structural characteristics of $CdMnO_3$ nanostructures prepared by this method is their crystallinity [7]. The perovskite-like structure is a common feature of manganite compounds. The perovskite structure of $CdMnO_3$ is characterized by a cubic or orthorhombic unit cell, depending on the synthesis conditions and post-deposition treatments [8,9]. The crystallite size usually ranges from a few nanometers to tens of nanometers, indicating the formation of nanocrystalline domains [10,11]. The high crystallinity of these nanostructures is crucial for their functional properties, as defects and grain boundaries can significantly impact their electronic and magnetic behavior [12,13].

The surface morphology of $CdMnO_3$ nanostructures often exhibits a dense and homogeneous distribution of nanoparticles or nanograins [14,15]. The co-sputtering technique allows for fine-tuning of the surface roughness and grain size by adjusting parameters such as sputtering power, oxygen partial pressure, and substrate temperature. For instance, higher substrate temperatures generally promote larger grain sizes and improved crystallinity, while lower temperatures may result in finer nanostructures with higher surface area, which is beneficial for catalytic applications [16-19].

The microscopic studies provide further insights into the microstructure of $CdMnO_3$ nanostructures. The well-defined lattice fringes often confirm the high crystallinity and single-phase nature of the material [20]. Selected-area electron diffraction (SAED) patterns typically exhibit sharp rings or spots, corresponding to the perovskite structure of $CdMnO_3$ [21]. Additionally, the stoichiometric composition of the nanostructures can be verified to ensure the desired Cd:Mn:O ratio is achieved [22].

Another important structural characteristic is the presence of defects, such as oxygen vacancies or cation disordering, which can significantly influence the material's properties. For example, oxygen vacancies are known to enhance the electrical conductivity and catalytic activity of manganites. The density of such defects can be controlled by varying the oxygen flow rate during the co-sputtering process or through post-deposition annealing in different atmospheres [23-25].

Recently, the research interests in cadmium manganite ($CdMn_2O_4$) have increased due to the effectiveness of this material in the fabrication of supercapacitors and Li-ion batteries [26]. As well, this

material was successfully used as an electrode material in electrochemical sensors of NO_x gases [27]. The $CdMn_2O_4$ nanostructures such as nanoparticles and nanofibers exhibit much better properties in such applications because of the drastic increase in surface-to-volume ratio [28]. Spinel cadmium manganite is described as a multifunctional material as the quantity and chemical identity of the Cd^{2+} ions can be tuned to obtain a wide range of properties [29]. The replacement of Mn^{2+} ions on the tetrahedral sites by Cd^{2+} ions mostly cause a large tetragonal distortion as a result of the Jahen-Teller effect [30]. The bulk $CdMn_2O_4$ is prepared by the solid state reaction method as the CdO and Mn_2O_3 powders are mixed and sintered at high temperatures (~900 °C) [31], while the $CdMn_2O_4$ nanostructures are mainly synthesized by electrospinning technique [32]. In both cases, the synthesized structures include compounds other than $CdMn_2O_4$.

The $CdMnO_3$ nanostructures prepared by DC reactive magnetron co-sputtering exhibit excellent crystallinity, controlled morphology, and tunable defect density, making them highly suitable for a wide range of applications. The ability to precisely control the structural characteristics of these materials through synthesis parameters underscores the versatility and potential of this fabrication technique.

In this work, highly-pure $CdMn_2O_4$ nanostructures were synthesized by reactive magnetron co-sputtering technique and the effect of mixing ratio on their structural properties was introduced.

2. Experimental Part

A dc sputtering system was used to prepare $CdMn_2O_4$ thin films on glass substrates. Two highly-pure targets of Cd and Mn were mounted on the cathode – as shown in Fig. (1) – to perform the co-sputtering process. The dimensions of targets were determined in light of the surface binding energies of both materials (2.92 eV for Mn and 1.16 eV for Cd) and the stoichiometry of the required compound. The diameters of Mn and Cd targets were 80 and 15mm, respectively. This configuration can ensure the stoichiometric reaction of Mn and Cd with oxygen atoms available in the discharge volume. A magnetron of 450G flux density was attached to the backside of the Mn target at the cathode to confine the ions near the target surface and hence increase the collisional ionization.

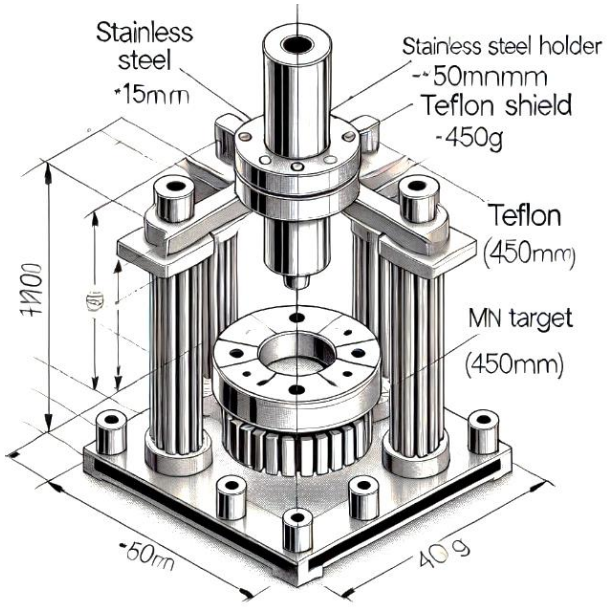

Fig. (1) Configuration of the Mn and Cd targets and magnetron on the cathode

The mixing ratio of argon and oxygen in the gas mixture can be precisely controlled by premixing these gases in a mixer before pumped into the discharge chamber. The total gas pressure reached 0.1 mbar. The cathode was cooled down to 4 °C in order to prevent the ion-induced secondary electron emission, while the anode was left to heat up to about 150 °C in order to induce the reaction between CdO and Mn_2O_3 particles and form the required compound ($CdMn_2O_4$).More details of the preparation conditions can be found elsewhere [33-36]. The nanopowders were extracted from thin film samples by conjunctional freezing-assisted ultrasonic extraction method [37-39].

The structural characteristics of the prepared thin films were determined by x-ray diffraction (XRD), scanning electron microscopy (SEM), energy-dispersive x-ray spectroscopy (EDS) and the Fourier-transform infrared (FTIR) spectroscopy.

3. Results and Discussion

Figure (2) shows the simulated XRD pattern of the $CdMn_2O_4$ samples prepared in this work. Figure (2a) shows the XRD pattern of the sample prepared using gas mixture of 1:1 and deposition time of one hour. All peaks belonging to the polycrystalline structure of $CdMn_2O_4$ are observed while no other peaks belonging to both CdO and Mn_2O_3 are seen in this pattern [40]. This initially highlights the structural purity of the prepared samples. Further tuning of the operation parameters and preparation conditions may lead to suppress some peaks and allow fewer number of crystal planes to grow. Using gas mixture of 2:1 and after 30 min of deposition, about half the number of peaks were suppressed as shown in Fig. (2b) and marked with the asterisk in table (1) as the amount of oxygen in the reaction volume was decreased as well as the time required for growth of more crystal planes. Table (1) shows the structural parameters of the prepared samples.

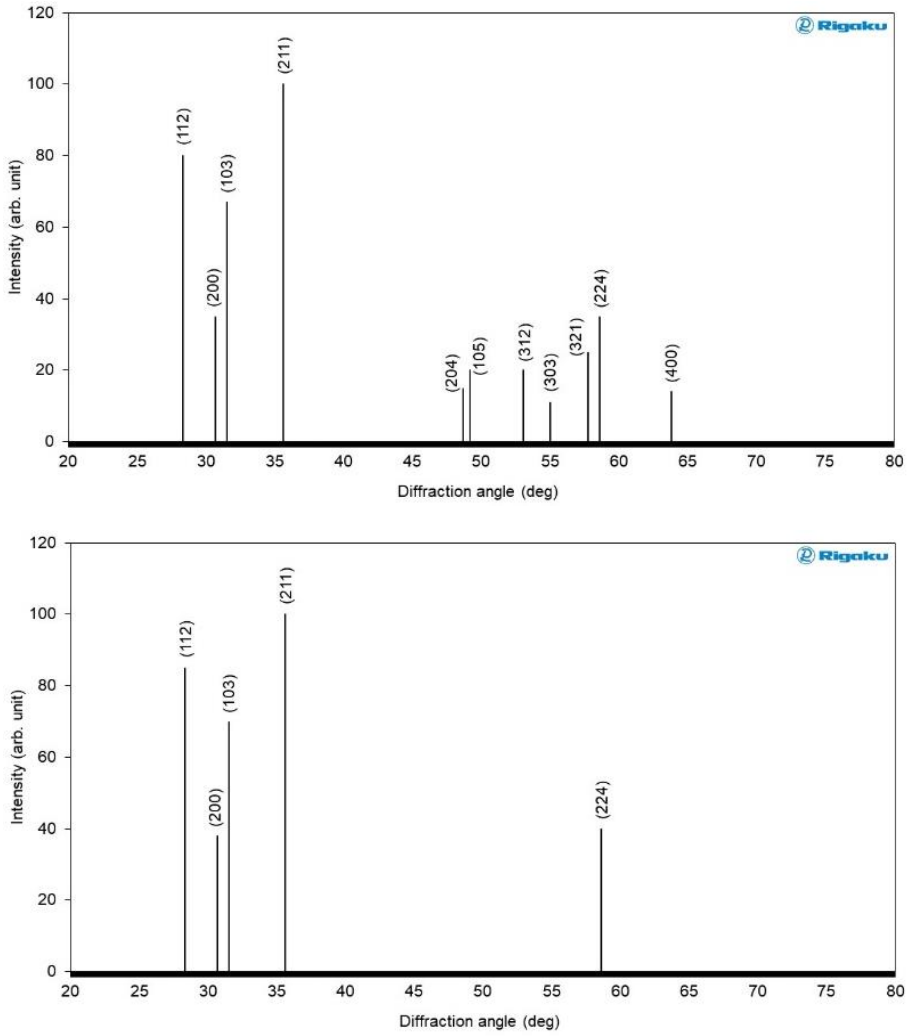

Fig. (2) Simulated XRD patterns of the $CdMn_2O_4$ samples prepared in this work using $Ar:O_2$ mixing ratio of 1:1 and deposition time of 60 min (upper) and 2:1 and 30 min (lower)

Figure (3) shows the FTIR spectrum of the $CdMn_2O_4$ samples prepared at different conditions in this work. As shown in Fig. (3a), three bands are observed at 451, 650 and 1304 cm^{-1}, which ascribed to the stretching vibrations of metal-oxygen (Mn-O, Cd-O and O-M-O) bonds [41-43]. No other bands are observed and this confirms the structural purity of the prepared samples. The two featured bands of metal-oxygen bond were seen in the sample prepared using gas mixture of 2:1 and deposition time of 30 min, while the band ascribed to the stretching vibration of O-M-O disappeared. Instead, a band

around 1590 cm^{-1}, which is ascribed to the vibration of O-H bond in water molecules, was seen. This may be attributed to the possible adsorption of water by the prepared sample.

Table (1) Structural parameters of the prepared samples determined from XRD results

2θ (deg.)	FWHM (deg.)	d_{hkl} (Å)	Crystallite size (nm)	(hkl)
28.147	0.303	3.519	27.02	(112)
30.951	0.562	3.525	14.66	(200)
31.026	0.519	2.375	15.88	(103)
35.852	0.692	3.525	12.06	(211)
48.357	0.173	3.518	50.32	(204)*
49.014	0.433	3.520	20.16	(105)*
53.167	0.649	3.502	13.68	(312)*
55.069	0.369	3.525	24.27	(303)*
58.297	0.512	3.757	17.76	(321)*
58.792	0.593	2.510	15.37	(224)
64.28	0.673	3.522	13.94	(400)*

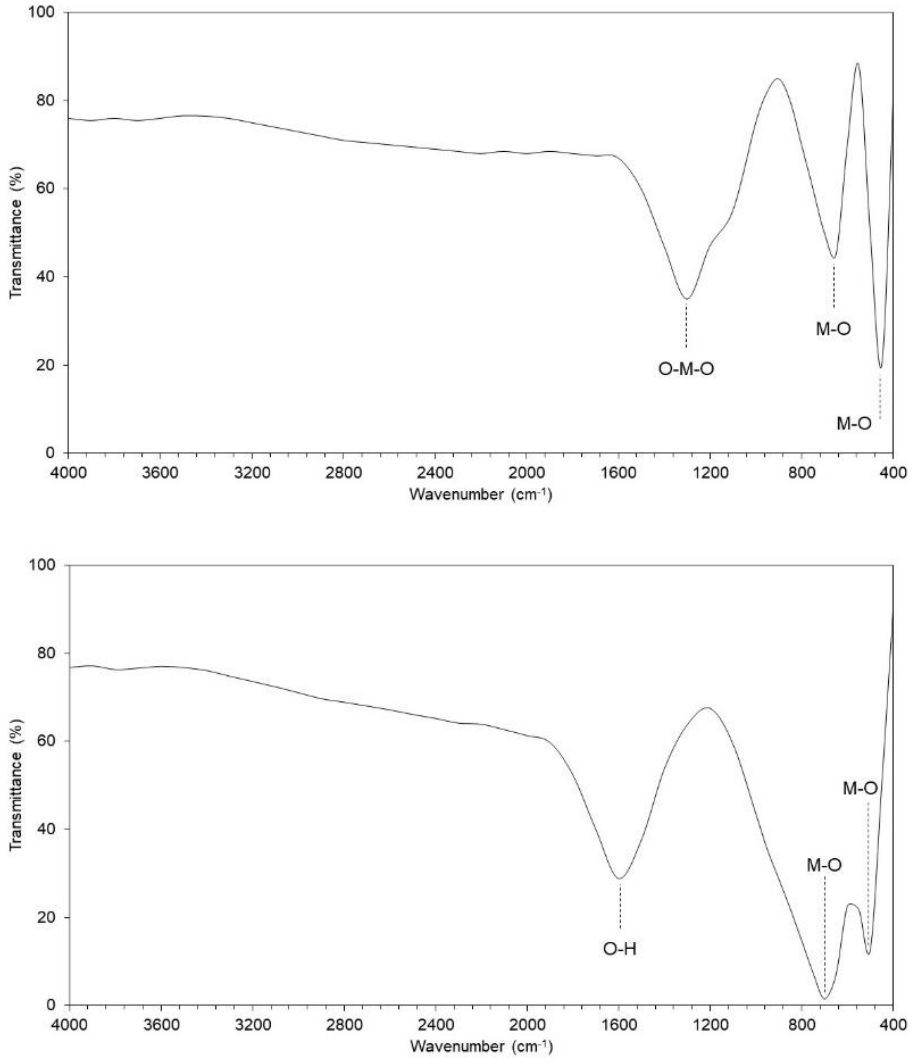

Fig. (3) FTIR spectra of the $CdMn_2O_4$ samples prepared in this work using $Ar:O_2$ mixing ratio of 1:1 and deposition time of 60 min (upper) and 2:1 and 30 min (lower)

In order to confirm the formation of nanostructures, figure (4a) shows the SEM image of the most-pure $CdMn_2O_4$ sample prepared in this work using gas mixture of 1:1 and deposition time of one hour. The minimum particle size is 20 nm, however, larger sizes are dominantly observed. The minimum particle size was not decreased further as the deposition time was reduced to 30 min. The stoichiometry

 ISSN (print) 2958-8960 (online) 3006-6042 Printed in IRAQ

of the prepared compound can be approved by the EDS result shown in Fig. (4b). No traces for other elements were found, which reflects the high structural purity of the prepared samples.

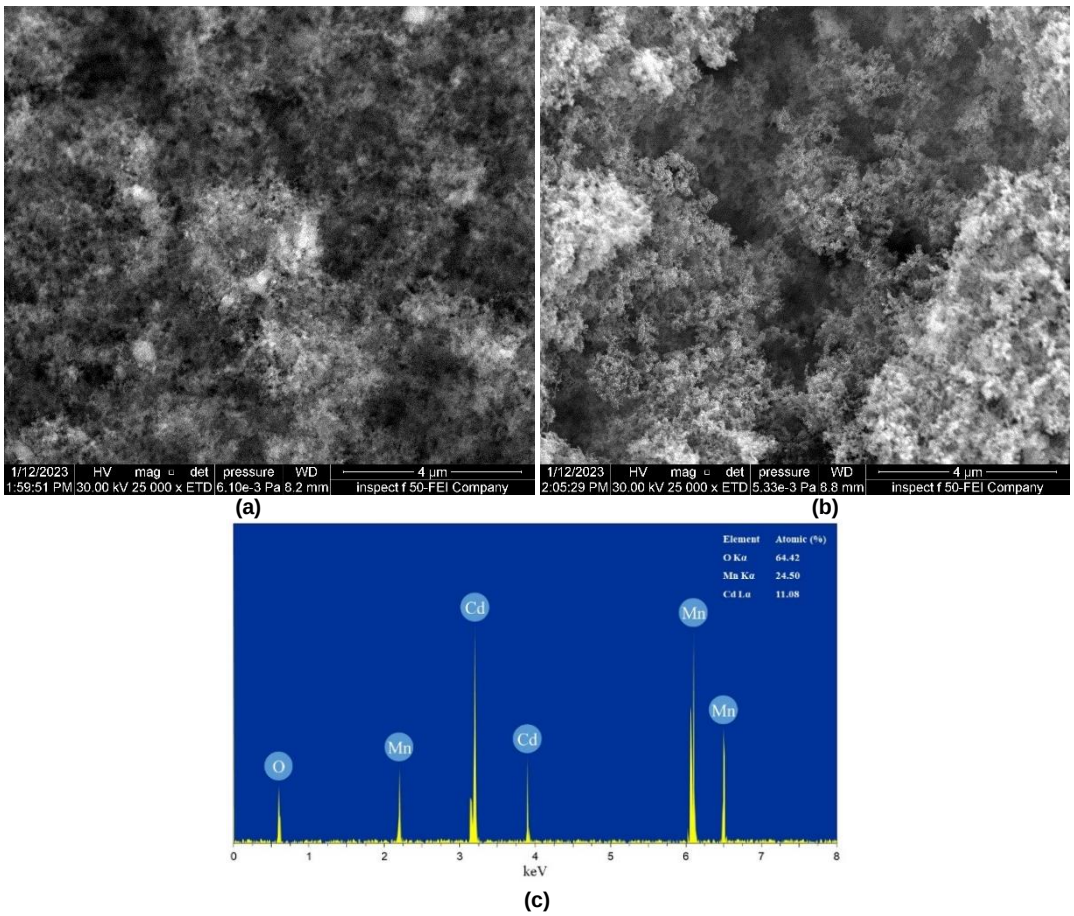

Fig. (4) SEM images of the $CdMn_2O_4$ sample prepared using (a) gas mixture of 1:1 and deposition time of 60 min, (b) 2:1 and 30 min, and (c) EDX spectrum for sample prepared using gas mixture of 1:1 and deposition time of 60 min

4. Conclusion

In concluding remarks, an attempt to prepare $CdMn_2O_4$ nanostructures by reactive magnetron co-sputtering technique. A new geometrical configuration was used for co-sputtering process depending on the dimensions of Cd and Mn targets with respect to each other. The mixing ratio of argon and oxygen was found very effective on the structural characteristics of the prepared nanostructures, those were highly pure as no elements other than cadmium, manganese and oxygen were found in the final sample. The growth of crystal planes in the prepared samples can be controlled by tuning the operation parameters and preparation conditions, especially gas mixing ratio and deposition time.

Conflict of Interest

Authors declare that they have no any conflict of interest related to this work.

References

[1] N. Miura, H. Kurosawa, M. Hasei, G. Lu, and N. Yamazoe, Solid State Ionics, 86–88(Pt 2) (1996) 1069-1073.
[2] J. Bhagwan, A. Sahoo, K.L. Yadav, and Y. Sharma, J. Alloys Comp., 703 (2017) 86-95.
[3] J. Bhagwan and J.I. Han, Ceram. Int., 50(14) (2024) 26086-26096.
[4] H.-J. Kim, C.-W. Kim, S.-Y. Kim, A.E. Reddy, and C.V.V. Muralee Gopi, Mater. Lett., 210 (2018) 143-147.
[5] X. Hao, T. Liu, W. Li, Y. Zhang, J. Ouyang, X. Liang, F. Liu, X. Yan, C. Zhang, Y. Gao, L. Wang, and G. Lu, Sens. Actuat. B: Chem., 302 (2020) 127206.
[6] C.B. Azzoni, M.C. Mozzati, L. Malavasi, P. Ghigna, and G. Flor, Solid State Commun., 119(10–11) (2001) 591-595.
[7] J.D. Hem and C.J. Lind, Geochimica Cosmochimica Acta, 55(9) (1991) 2435-2451.
[8] S.D. Sarker and L. Nahar, “Characterization of nanoparticles”, Ch. 3, A.D. Talukdar, S.D. Sarker, J.K. Patra (ed.), in Nanotechnology in Biomedicine, Advances in Nanotechnology-Based Drug Delivery Systems, Elsevier (2022), pp. 45-82.
[9] M. Ramstedt, C. Norgren, A. Shchukarev, S. Sjöberg, and P. Persson, J. Colloid Interface Sci., 285(2) (2005) 493-501.

[10] E.V. Vladimirova, B.V. Slobodin, and L.L. Surat, Russian J. Inorg. Chem., 45(10) (2000) 1594-1597.
[11] J.P. Araújo, V.S. Amaral, P.B. Tavares, F. Lencart-Silva, A.A.C.S. Lourenço, E. Alves, J.B. Sousa, and J.M. Vieira, J. Magnet. Magnet. Mater., 226-230 (Pt1) (2001) 797-799.
[12] V. Gupta, B. Raina, and K.K. Bamzai, J. Mater. Sci.: Mater. Electron., 29(11) (2018) 8947-8957.
[13] X.-F. Zeng, Z.-W. Wang, X.-M. Yu, X.-X. Wang, T. Li, Z.-H. Ji, Y.-Y. Hou, H. Zhang, abd Z. Xu, Geology in China, 38(1) (2011) 212-217.
[14] A.P.B. Sinha, N.R. Sanjaxa, and A.B. Biswas, New Cryst. Struct., 109(1-6) (1957) 410-421.
[15] V. Gupta, B. Raina, D. Singh, and K.K. Bamzai, Integ. Ferroelectr., 185(1) (2017) 165-175.
[16] S.K. Dey and J.C. Anderson, Philos. Mag., 12(119) (1965) 975-984.
[17] L. Bochatay, P. Persson, and S. Sjöberg, J. Colloid Interface Sci., 229(2) (2000) 584-592.
[18] G.G. Robbrecht and C.M. Henriet-Iserentant, phys. stat. sol. (b), 41(1) (1970) K43-K46.
[19] V. Gupta, B. Raina, S. Verma, and K.K. Bamzai, AIP Conf. Proc., 1953 (2018) 050010.
[20] K.M. Abdul Shekkeer, K.Y. Cheong, and H.J. Quah, Int. J. Energy Res., 46(11) (2022) 14814-14826.
[21] J. Deng and H.J. Quah, Int. J. Nanotechnol., 21(4-5) (2024) 324-338.
[22] N. Ishigaki, N. Kuwata, A. Dorai, T. Nakamura, K. Amezawa, and J. Kawamura, Thin Solid Films, 686 (2019) 137433.
[23] S.E. Nunes, L.C. Matte, and C.R. Da Cunha, Mater. Res. Exp., 6(9) (2019) 095905.
[24] P.H.M.A. Hedei, Z. Hassan, and H.J. Quah, Int. J. Nanotechnol., 19(2-5) (2022) 211-222.
[25] P.H.M.A. Hedei, Z. Hassan, and H.J. Quah, Appl. Surf. Sci., 550 (2021) 149340.
[26] H.R. Moazami, S.S. Hosseiny Davarani, N. Ghassemi and S. Hamed, J. Solid State Electrochem., 24 (2020) 1231-1238.
[27] J. Bhagwan, A. Sahoo, K.L. Yadav and Y. Sharma, J. Alloys Compd., 703 (2017) 86-95.
[28] S.G. Porji, V.A. Thakur and B.A. Mulla, Proc. Indian Natur. Sci. Acad., 61(3-4) (1995) 229-235.
[29] G.N.P. Oliveira, R. Teixeira, T.M. Mendonça, M.R. Silva, J.G. Correia, A.M.L. Lopes and J.P. Araújo, J. Appl. Phys., 116(22) (2014) 223907.
[30] P. Ghigna, G. Flor and G. Spinolo, J. Solid State Chemi.,149(2) (2000) 252-255.
[31] S.K. Dey, Phys. Lett., 22(4) (1966) 375-377.
[32] I.O. Troyanchuk, H. Szymczak and N.V. Kasper, phys. stat. sol. (a), 157(1) (1996) 159-166.
[33] O.A. Hammadi, M.K. Khalaf and F.J. Kadhim, Opt. Quantum Electron., 47(12) (2015) 3805-3813.
[34] E.A. Al-Oubidy and F.J. Al-Maliki, Iraqi J. Appl. Phys., 14(4) (2018) 19-23.
[35] F.J. Al-Maliki, O.A. Hammadi and E.A. Al-Oubidy, Iraqi J. Sci., 60 (Special Issue) (2019) 91-98.
[36] F.J. Al-Maliki and E.A. Al-Oubidy, Physica B: Cond. Matter, 555 (2019) 18-20.
[37] O.A. Hammadi, Proc. IMechE, Part N, J. Nanomater. Nanoeng. Nanosys., 232(4) (2018) 135-140.
[38] O.A. Hammadi, Plasmonics, 15(6) (2020) 1747-1754.
[39] O.A. Hammadi, Iraqi J. Appl. Phys., 15(4) (2019) 23-28.
[40] Standard X-Ray Diffraction Powder Patterns, Section 10, National Bureau of Standards, Monograph 25 (1972) p. 16.
[41] N.N. Greenwood and E.J.F. Ross, “Index of Vibrational Spectra of Inorganic and Organometallic Compounds”, vol. I, Butterworth Group (London, 1960), p. 326, 328.
[42] N.N. Greenwood and E.J.F. Ross, “Index of Vibrational Spectra of Inorganic and Organometallic Compounds”, vol. II, Butterworth Group (London, 1963), p. 457.
[43] N.N. Greenwood and E.J.F. Ross, “Index of Vibrational Spectra of Inorganic and Organometallic Compounds”, vol. III, Butterworth Group (London, 1966), p. 800, 1078.

